Cement & Concrete Composites 32 (2010) 300–311

Contents lists available at ScienceDirect

Cement & Concrete Composites

journal homepage: www.elsevier.com/locate/cemconcomp

Prediction of potential compressive strength of Portland clinker from its mineralogy

K. Svinning [a,*], A. Høskuldsson [b], H. Justnes [c]

[a] NORCEM A/S, Process and Environmental Department, Brevik, Norway
[b] Centre for Advanced Data Analysis, Eremitageparken 301, 2800 Kgs Lyngby, Denmark
[c] SINTEF Building and Infrastructure, Concrete, Trondheim, Norway

ARTICLE INFO

Article history:
Received 5 February 2009
Received in revised form 15 December 2009
Accepted 15 December 2009
Available online 28 December 2009

Keywords:
Portland clinker
Potential compressive strength
Mineralogy
XRDA
Prediction
PLS

ABSTRACT

Based on a statistical model first applied for prediction of compressive strength up to 28 d from the microstructure of Portland cement, potential compressive strength of clinker has been predicted from its mineralogy. The prediction model was evaluated by partial least squares regression. The mineralogy was described by patterns from X-ray diffraction analysis in the 2θ-regions 29.88–30.70° and 32.90–34.10° (using CuKα-radiation).

It has been shown that prediction of potential compressive strength of clinker up to 28 d from the observed variation in the mineralogy gave a significant variation of the strength at both 1 and 28 d. Sensitivity analysis based on simulation, optimisation and prediction made it possible to study the influence of the mineralogy on the strength in more detail.

1. Introduction

The influence of the characteristics or the microstructure of Portland cement on compressive strength up to 28 d was investigated statistically by Svinning et al. [1] by application of multivariate data analysis, specifically partial least square regression (PLS) analysis. The main groups of characteristics were mineralogy and superficial microstructure represented by curves from X-ray diffraction analysis (XRDA) and differential thermogravimetric analysis (DTGA), as well as particle size distributions. PLS gave maximum explained variance in compressive strength at 1, 2, 7 and 28 d of 93%, 90%, 79% and 67%, respectively. Most of the variance in the compressive strength up to 28 d was explained from the variances of the variables describing the mineralogy and the particle size distribution. The variables describing the superficial microstructure influenced the compressive strength at 28 d less than the compressive strength at 1 d.

Clinkers from four Scandinavian plants were examined with respect to microstructure and cement properties by Svinning et al. [2]. The development of clinker's potential compressive strength up to 28 d was predicted from its microstructure. Two methods were used to characterise the microstructure of clinker, scanning electron microscopy (SEM) and X-ray diffraction analysis (XRDA). When analysing the process condition in a kiln from the microstructure of clinker, it was found that characterisation of the microstructure by SEM gave more valuable information than characterisation by XRDA. The microstructure characterised by SEM reflected different heating and cooling rates, due to the different size of the kilns and the different types of coolers. XRDA of the cement on the other hand, gives satisfactory characterisation of the mineralogy of the clinker part of the cement concerning the prediction of the compressive strength of cement. The mineralogy of the clinker is described in Refs. [1,2] by XRD-profiles in the 2θ – ranges 29.88–30.70° and 32.90–34.10° (using CuKα-radiation).

The mineral composition could be determined by multi-component Rietveld analyses. Instead of including selected parts of the diffractogram, which requires many variables to describe the profiles, only a few variables giving the whole mineral composition would need to be included in PLS. However, the inaccuracy of the amount of a mineral determined by Rietveld analyses will increase as the amount of the mineral decreases. C_3A could also exist as two polymorphs, cubic and orthorhombic, with different reactivity. A total amount of C_3A, as calculated by the Bogue methodology, like for instance 5%, split into polymorphs could lead to a fairly high inaccuracy in the calculation of the amount of each. The benefits of including the XRD-profile as it has been done here are: (a) no information is lost, and (b) any change in structure or unit cell dimensions due to foreign ion contamination or interchange will be detected directly by changes in the position of the respective peaks. Such structural changes of the minerals may influence their reactivity towards water leading to changes in properties like compressive strength up to 28 d as shown by Svinning et al. [2].

* Corresponding author. Tel.: +47 35572314; fax: +47 35570400.
E-mail address: ketil.svinning@norcem.no (K. Svinning).

0958-9465/$ - see front matter © 2009 Elsevier Ltd. All rights reserved.
doi:10.1016/j.cemconcomp.2009.12.004

As discussed in [1], the range 2θ = 29.88–30.70° contains information solely on alite and aphthitalite, $K_3Na(SO_4)_2$ (i.e. other known cement minerals have no reflections in this region). Although the intensities of the two overlapping alite reflections are modest, the domination of this mineral in Portland cement secures a good signal-to-noise ratio for this mineral. Alite is dominating the early strength development, as is well known. One of the strongest reflections of aphthitalite is in the high end of this first XRD region, and it can give valuable information on this easily soluble alkali sulphate. In spite of its low content, aphthitalite can dominate the early pore water chemistry and strongly influence setting time, for instance. The second XRD region of 2θ = 32.90–34.10° is dominated by reflections of C_3A and C_4AF, but it also contains the dominating reflection of the more seldom clinker minerals α'-C_2S and mayenite, $C_{12}A_7$. The common clinker phase belite, β-C_2S, also has a modest reflection in the low end of this region. However, since alite and belite are the only silicate phases, an increase in alite content will lead to a decrease in belite content so an independent control of the latter is not required. Thus, the two selected XRD regions cover the responses for all the important clinker minerals, and they measure more directly the actual content of each mineral since the simple Bogue calculation is at best an indication of the mineral composition.

Knöfel [3] established a formula for predicting compressive strength at 28 d as a function of clinker phases. The strength increased most with the portions of alite and less by the portions of belite and aluminate. The strength decreased with an increase in the portion of ferrite. Lawrence [4] has established a formula for predicting compressive strength at 1 d. The predicted strength increased with the amount of C_3S and decreased with decreasing amounts of C_3A and C_4AF. According to Aldridge [5], the influence of C_3S decreases with increasing age of curing while the influence of C_2S increases. Odler and Wonnemann [6,7] have studied the effect of alkalis on Portland cement hydration. In [6] the effect of alkali oxides incorporated into the crystalline lattice of clinker minerals was studied and in [7] the effect of alkalis present in form of sulfates.

Ono developed methods to interpret kiln conditions and formulae to predict 28-d mortar-cube strength (F28d). Ono's latest formula [8] express *F*28*d* as a function of alite size, alite birefringence, belite size and belite color. The equation should be modified in case of magnesia content higher than 1.8% and lower than 1.2%. According to Ono [9] the alite birefringence will vary with lattice constants of alite, which again will vary with the amount of SO_3 and magnesia as well as with the burning temperature and hydraulic activity. From this, he concluded that the X-ray powder diffraction analysis may be an alternative method to microscopy with respect to characterising and controlling the quality of clinker. Tricalcium silicate exhibits seven polymorphs depending on the impurities and the temperature: T_1, T_2, T_3 for the three triclinic forms, M_1, M_2, M_3 for the three monoclinic forms and *R* for the rhombohedral one [10]. The most common modifications are M_1 and M_3. The formation temperature for M_3 is higher than for M_1. Maki and Chromy [11] have shown that M_1 and M_3 can be distinguished by means of birefringence measurements.

Portions of XRD powder patterns of the different modifications of C_3S were presented by Maki and Kato [12]. The 2θ ranges of the patterns being focused were 32–33° and 51–52°. The peak at approximately 32.6° could contribute much for explaining the change in compressive strength from the change in the birefringence of alite. The profile of the peak rather than its position is changing with the modification from M_3 to M_1. The peak position seems, however, to move slightly to a lower 2θ angle with an increase in M_3 and a decrease in M_1. In a XRD powder pattern of cement, the C_3S-peak at 32.6° will overlap a peak of belite, which will make interpretation of the XRD pattern even more complicated. The positions at 2θ angles 30.04° and 32.6° are reported to change simultaneously and similarly [13]. The ranges of 2θ angle 29.92–30.70° and 32.90–34.10° could therefore be defined to contain sufficient information about the structure of alite for predicting potential compressive strength.

Besides ordinary multivariable regression, fuzzy logic [14], stepwise regression [15], genetics algorithms–artificial neural networks (GAs–ANNs) [16], gene expression programming (GEP) and neural networks (NNs) [17] and PLS [2,18–21] have been applied in the evaluation of the model for prediction of cement strength. GAs–ANNs and PLS represent different types of multivariate calibration or modelling with hidden layer or latent variables. In [21], the latent variables were taken into consideration in the sensitivity analysis while in [16] the hidden layers were not. In [21], examples of sensitivity analysis in the form of a simulated variation of a latent variable from which cement properties are predicted are shown. In the [14–17], only variables presenting chemical component composition not the mineralogy of clinker were included in the modelling.

The prediction of potential compressive strength of clinker from the mineralogy was in this work based on a PLS model evaluated for prediction of compressive strength by Svinning et al. [1] from the whole microstructure of the cement. The observation **X**-matrix could be partitioned into the sub-matrices: $\mathbf{X}_{\text{mineralogy}}$, $\mathbf{X}_{\text{part distr}}$, $\mathbf{X}_{\text{superficial micr LT}}$ and $\mathbf{X}_{\text{superficial micr HT}}$ (LT and HT refer to the low and high temperature range differential thermogravimetric analysis (DTGA)) .The potential compressive strength was predicted from an artificial observation matrix where all the variables, except $\mathbf{x}_{\text{mineralogy}}$ presented as the XRD intensities in the two 2θ ranges, were kept constant and equal to their mean values. The number of observations was the same as in the original observation matrix.

The influence of the mineralogy on the potential compressive strength was examined by simulation, optimisation and prediction. The latent structure of XRD intensities is found by evaluating a new PLS model for predicting potential strength from the XRD intensities only. Variation in the intensities was simulated by model-based optimisations of $\mathbf{x}_{\text{mineralogy}}$ to achieve compressive min and max strength at either 1 or 28 d. It was concluded in [21] that the influence of a latent variable on *y* was much more significant than that of a single *x*-variable. Optimisation of *y* constrained by PLS-components will therefore give a more realistic and better solution for implementation in the design of cement and the quality control during production.

Finally, the potential compressive strengths at 1, 2, 7 and 28 d was predicted from the simulated variation in the intensities being a part of a full *x*-variables observation matrix where all the other *x*-variables were kept constant and equal to their mean values. This type of sensitivity analysis has been presented by Svinning and Høskuldsson [21,22]. The amounts of Na_2O and K_2O and the ratio Al_2O_3/Fe_2O_3 were included as supplementary variables from the interest of studying the influence of these variables on the structure of the clinker minerals.

2. Methods

2.1. Characterisation of mineralogy of clinker

The XRD analysis was performed on ground clinker. The XRD-profiles consisted of intensities at every 0.02°. The scaling of the intensities and adjustment of the 2θ-position of the diffraction peaks were based on normalisation of the area and adjusting the 2θ-axis to match the diffraction peak at d = 3.52 Å for anatase (TiO_2), which was intermixed in an amount of 10 wt.% of the total sample. Examples of diffractograms including the peak of the reference are shown in Fig. 1. To reduce the number of intensities (and

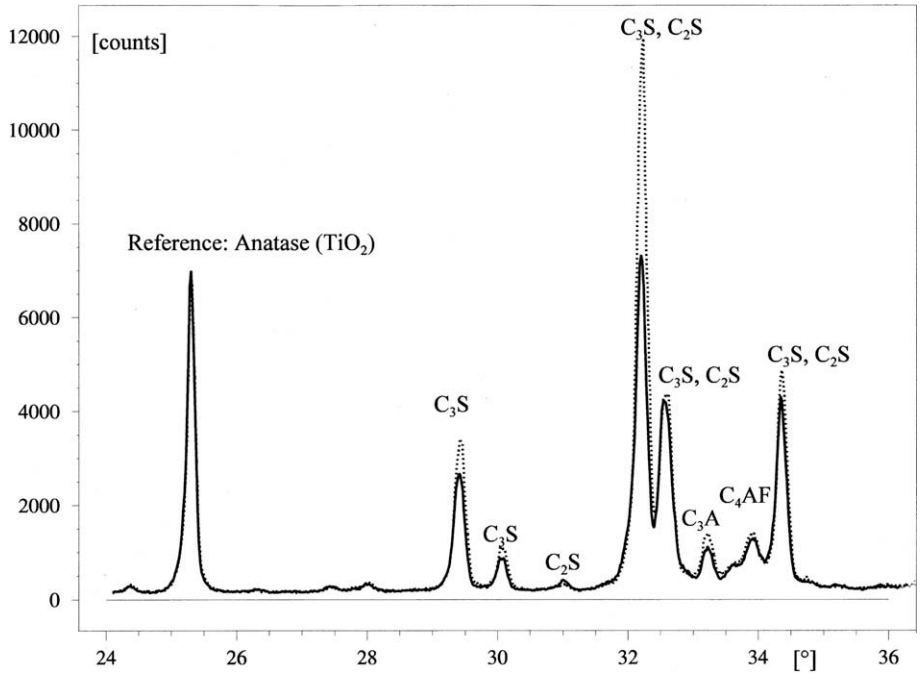

Fig. 1. Examples of X-ray diffractograms of two neat cements in the 2θ range 24–36° (from Ref. [1]).

the number of variables) and simultaneously increase the signal-to-noise ratio, one variable was made out of three by averaging three adjacent variables in the diffraction profile before including the variables in PLS. The number of variables was further decreased by selecting two small regions (2θ) of diffractogram, 29.88–30.70° and 32.90–34.10° (using CuKα-radiation), to be included in the modelling.

The brand of the diffractometer used was Philips X'pert. The TG apparatus applied was a Netzsch STA – Apparatur 409 V/3/C®.

2.2. Evaluation of the prediction model

In cases where the number of variables is large relative to the number of observations or objects, data compression by expressing the original *x*-variables by fewer latent variables or factors could be necessary. Partial least square regression (PLS) performs calculation and optimisation of a number of factors for maximum explanation of variance in the *y*-variables. In addition, model parameters are calculated for prediction of y for new values of the *x*-variables. In this work PLS was performed on several *y*-variables combined expressed as a vector. The models which relate the PLS model terms are given by the two expressions in the equations below:

$$\mathbf{X} = \mathbf{T}\mathbf{P}^T + \mathbf{E} \tag{1}$$

$$\mathbf{Y} = \mathbf{U}\mathbf{Q}^T + \mathbf{F} \tag{2}$$

T and **U** are factor scores, **P** and **Q** are *x* and *y*-variables loadings and **E** and **F** are the residuals in **X** and **Y**, respectively. Alternatively, Eq. (1) could be expressed in the form:

$$\mathbf{X} = \mathbf{t}_1\mathbf{p}_1^T + \mathbf{t}_2\mathbf{p}_2^T + \cdots + \mathbf{t}_a\mathbf{p}_a^T + \cdots + \mathbf{t}_A\mathbf{p}_A^T + \mathbf{E} \tag{3}$$

A is equal to the maximum number of latent variables for maximum explanation of variance in **Y**.

By scaling the variables, unreasonable domination of variables with dominating standard deviations, $s(\mathrm{x})$, on the model can be avoided. The weighting of $x_{i,k}$ by centering and scaling is performed according to the following formula:

$$x_{ik,w} = \frac{x_{ik} - \bar{x}_k}{s(x_k)} \tag{4}$$

The iterative algorithms for calibration, validation and prediction are described in detail in Martens and Næs [23].

2.3. Sensitivity analysis

The type of sensitivity analysis to be applied for examining the influence of *x* on *y* depends greatly on the type of modelling applied. In multivariate data analysis like for example PLS, *y* is correlated to the latent variables which are linear combinations of the *x*-variables (Eq. (3)). In [3] the variation in *y* is predicted from simulated variation of a latent variable. The latent variable may be a combination of several original latent variables.

The influence of *x*-variables on the *y*-variable(s) may be evaluated by predicting variation in *y* or *y* from variation of one latent variable at a time from one 'observed' extreme to the other. By varying the *a*'th latent variable $\Delta t\,\mathbf{p}_a$ the variation in Δx_k in its original form, i.e. not scaled, can be calculated in the following way:

$$\Delta x_k = (\Delta t p_{ka}) s(x_k) \tag{5}$$

Similar to a type of sensitivity analysis with variation of only one *x*-variable, the score, *t*, is varied in one direction and in equal steps, Δt. Calculation of x_j, neither centered nor scaled, will be as follows:

$$x_k = (t p_{ka}) s(x_k) + \bar{x}_k \tag{6}$$

Variation in the whole observation **X**-matrix was usually simulated prior to the prediction by constructing an artificial observation **X**-matrix. In some cases, sensitivity analysis in the form of prediction from simulated variation of a selection or a group of variables could be appropriate.

An influence of one or several *x*-variables on a *y*-variable is defined in this work as being significant if there is no overlap of confidence intervals of $\hat{y} \pm 1s(\hat{y}_k)$ of predicted maximum and minimum *y*, respectively.

The simulation of the variation of the mineralogy, by varying XRD intensities in selected 2θ – ranges, could be based on variation

of one or several latent variables of the XRD intensities. The examination of the influence was carried out in the following way:

In an overall model

$$y = \mathbf{b}^T \left(\mathbf{x}_{\text{mineralogy}} \mid \mathbf{x}_{\text{part distr}} \mid \mathbf{x}_{\text{superficial micr LT}} \mid \mathbf{x}_{\text{superficial micr HT}} \right) + b_0 \tag{7}$$

where the sub-matrices represent the different parts of the microstructure, the examination of the influence of $\mathbf{x}_{\text{mineralogy}}$ on y is carried out by the following procedure:

1. Prediction of $\hat{y}$ from

$$\left(\mathbf{X}_{\text{mineralogy}}(M \times K_{\text{mineralogy}}) \;\middle|\; \begin{matrix} (\bar{\mathbf{x}}_{\text{part distr}})_1 \\ \vdots \\ (\bar{\mathbf{x}}_{\text{part distr}})_M \end{matrix} \;\middle|\; \begin{matrix} (\bar{\mathbf{x}}_{\text{superficial micr LT}})_1 \\ \vdots \\ (\bar{\mathbf{x}}_{\text{superficial micr LT}})_M \end{matrix} \;\middle|\; \begin{matrix} (\bar{\mathbf{x}}_{\text{superficial micr HT}})_1 \\ \vdots \\ (\bar{\mathbf{x}}_{\text{superficial micr HT}})_M \end{matrix} \right)$$

where M is the number of rows in the observation $\mathbf{X}$-matrix

2. Revealing the latent structure of $\mathbf{x}_{\text{mineralogy}}$ can be done by evaluating a new model $y = \hat{y} = \mathbf{b}^T(\mathbf{x}_{\text{mineralogy}} \quad \mathbf{x}_{\text{suppl var}}) + b_0$ using PLS. $\mathbf{x}_{\text{suppl var}}$ may contain a few supplementary variables relevant for interpretation of variation in $\mathbf{x}_{\text{mineralogy}}$.
3. Simulation of variation in $\mathbf{x}_{\text{mineralogy}}$ by varying one or several latent variables and establishing an artificial observation matrix $\mathbf{X}_{\text{mineralogy}}(M, \text{art} \times K_{\text{mineralogy}})$ with M, art rows where $M, \text{art} < M$ and $M-1$, art is the number of changes in equal steps of $\mathbf{x}_{\text{mineralogy}}$
4. Prediction of $\hat{y}$ from

$$\left(\mathbf{X}_{\text{mineralogy}}(M, \text{art} \times K_{\text{mineralogy}}) \;\middle|\; \begin{matrix} (\bar{\mathbf{x}}_{\text{part distr}})_1 \\ \vdots \\ (\bar{\mathbf{x}}_{\text{part distr}})_{M,\text{art}} \end{matrix} \;\middle|\; \begin{matrix} (\bar{\mathbf{x}}_{\text{superficial micr LT}})_1 \\ \vdots \\ (\bar{\mathbf{x}}_{\text{superficial micr LT}})_{M,\text{art}} \end{matrix} \;\middle|\; \begin{matrix} (\bar{\mathbf{x}}_{\text{superficial micr HT}})_1 \\ \vdots \\ (\bar{\mathbf{x}}_{\text{superficial micr HT}})_{M,\text{art}} \end{matrix} \right)$$

The simulation was performed by minimizing and maximizing y by application of linear programming. The constraints were given by a latent variable or principal component and lower and upper limits of total variation of $\mathbf{x}$. In the simulation above M, art was set equal to 2.

In order to achieve the most optimal solution, several PLS-components could be involved in the optimisation. The "loadings" in the new constraints are linear combinations of the original ones and could be expressed as follows:

$$\mathbf{p}_{\text{combination of several PLS-components}} = \sum_{a=1}^{A} n_a \mathbf{p}_a \tag{8}$$

where $\sum_{a=1}^{A} n_a = 1$ and $0 < n_a < 1$.

The latter constraint prevents absolute values of the scores, |t|, of optimal $\mathbf{x} = (x_1\, x_2 \cdots x_K)$ to be unreasonably high. The model-based optimisation is described in more detail by Svinning et al. [22].

3. Experimental

The types of clinker included in the investigation are applied in the production of the following cements, with reference to European (EN) and in addition Norwegian standards (NS) where they differ by national addendum:

1. Low alkali, sulphate resistant cement, EN 197-1-CEM I 42.5 R, NS 3086-CEM I R-SR-LA
2. Low alkali, high strength cement, EN 197–1-CEM I 52.5 N, NS 3086-CEM I 52.5 N-LA
3. Standard Portland cement, EN 197-1-CEM I 42.5 R
4. Rapid Portland cement, EN 197-1-CEM I 42.5 R, NS 3086-CEM I 42.5 RR.

Table 1 contains the typical mineral composition (calculated from the chemical composition by Bogue's formula) in the clinker used in the different types of cement presented above.

Some of the samples of standard Portland cement, EN 197–1-CEM I 42.5 R, contained limestone filler.

The original observation $\mathbf{X}$-matrix consisted of 146 observations and 210 variables. The x-variables were divided into the following groups or categories:

1. Mineralogy of the clinker part of the cement described by X-ray diffractogram sequences (2θ-angle) 29.88–30.70° and 32.90–34.10° (using CuKα-radiation) were taken as variables no. 1–14 and 17–32.
2. Variables no 38–106 and 137–213 were the superficial microstructure of the cement as described by thermograms from DTGA
3. Particle size distribution of the cement were taken into account by variables no. 110–136
4. Variable no. 15–16 consisted of the amount of SO_3 and free lime
5. Variables not included in basic modelling but later included in the sensitivity analysis. These variables were the amounts of K_2O and Na_2O, respectively, and the ratio Al_2O_3/Fe_2O_3.

Table 1
Typical mineral composition of the clinker used in the different types of cement presented above.

Mineral and chemical comp. [%]	Sulphate resistant	High strength	Standard Portland	Rapid Portland
C_2S	16	12	13	12
C_3S	60	66	65	66
C_3A	0.5	6.1	7.7	6.1
C_4AF	15.8	11.0	10.0	11.0
Free lime	0.8	1.1	1.3	1.4
Na_2O-equiv.	0.53	0.55	1.05	1.15

The original *y*-variables: Compressive strengths at 1, 2, 7 and 28 d, were measured according to EN 196-10. For predicting potential strength of clinker, only the variables describing the mineralogy were varied. The intensity defined to be measured at $2\theta = 29.92^{\circ}$ was the average of the intensities measured at $2\theta = 29.88$, 29.90 and 29.92, the intensity defined to be measured at $2\theta = 29.98^{\circ}$ was the average of the intensities measured at $2\theta = 29.88$, 29.90 and 29.92 and so forth.

The software applied for PLS was Unscrambler version 9.7 and for optimisation OptPilot [22].

4. . Results and discussion

4.1. Prediction of potential compressive strength of clinker from observed mineralogy of the clinker part of the cement

Prior to the investigation of the influence of the mineralogy of the clinker on the compressive strength by sensitivity analysis, the variation of potential compressive strength was predicted from the observed variation in the mineralogy of the clinker part of cement. The significance of the variation of the predictive strength can be studied by comparing the variation in the predicted strength with the standard deviation of each of the predicted strengths. Fig. 2 shows the mean values of the variables describing the particle size distribution of the cement, and Figs. 3 and 4 show the mean values of the variables describing the superficial microstructure. Giving a simpler overview of the variation in the XRD-profiles, every fifth observation is depicted in Fig. 5. To predict the potential compressive strength, the values of the variables describing the other parts of the microstructure were defined and fixed. In this case the values are set constant and equal to their mean values. Fig. 6 shows the regression coefficients **b**: $b_1, b_2, \cdots b_K$ used in the prediction model $y = b_0 + \sum_{k=1}^{K} b_k x_k$ for prediction of the four *y*-variables for prediction of compressive strength from the XRD-profiles in Fig. 5. Figs. 7 and 8 show the predicted compressive strength at 1 and 28 d, respectively, including confidence intervals of $\hat{\mathbf{y}}_i \pm s(\hat{\mathbf{y}}_i)$.

The confidence intervals of the predicted potential compressive strength of clinker at 28 d are larger than the confidence intervals of the predicted potential strength at 1 d, and also larger relative to the range of variation of the predicted potential compressive strength. This is in accordance with the results in [1] which show that the predicted versus measured compressive strength at 1 d fits the target line (predicted equal to measured) better than the compressive strength at 28 d. There is no overlap of the confidence intervals of minimum and maximum of strengths at either 1 or

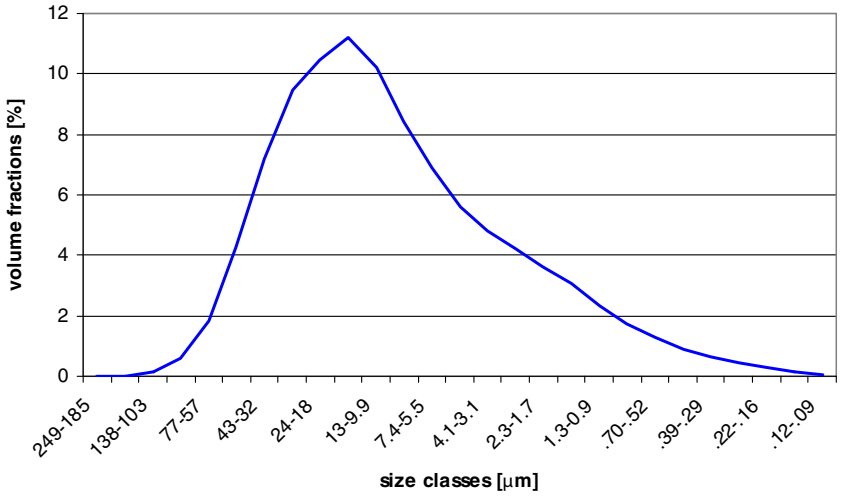

Fig. 2. Mean values of the variables describing the particle size distribution.

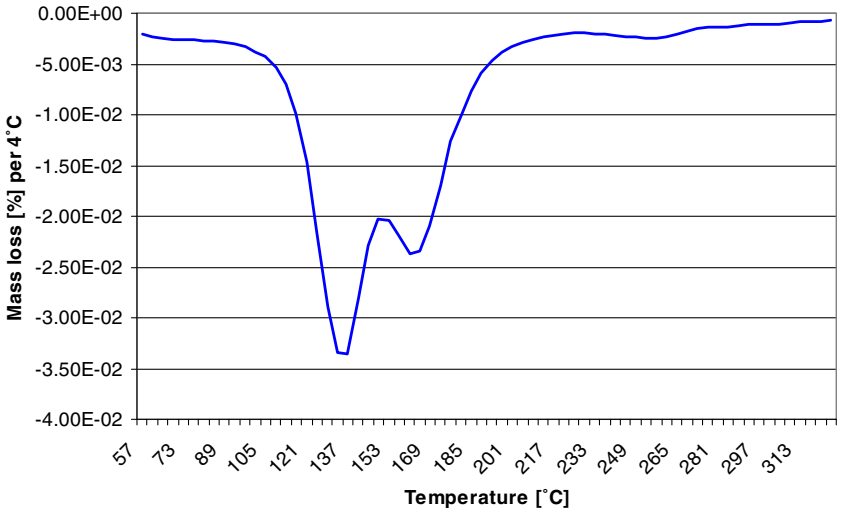

Fig. 3. The mean values of the variables from DTGA, describing the superficial microstructure; the degree of dehydration of gypsum and prehydration of the clinker minerals.

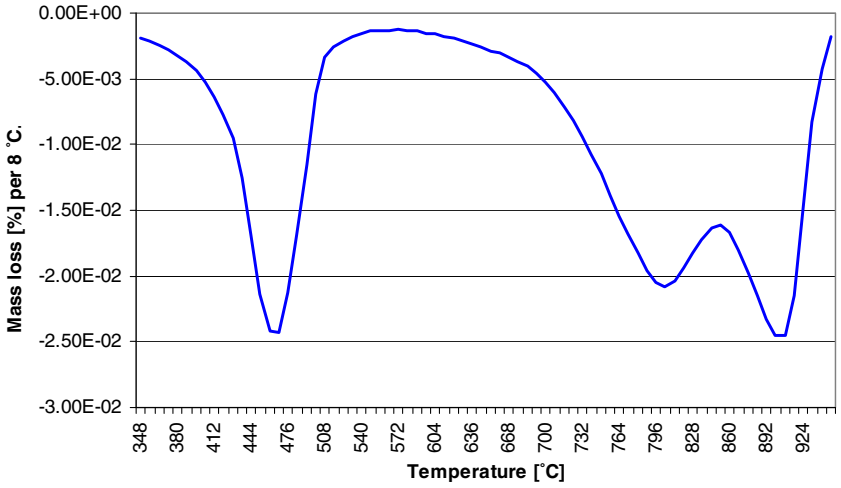

Fig. 4. The mean values of the variables from DTGA, describing the superficial microstructure; the degree of prehydration of free lime, carbonation of $Ca(OH)_2$ and the amount of limestone filler.

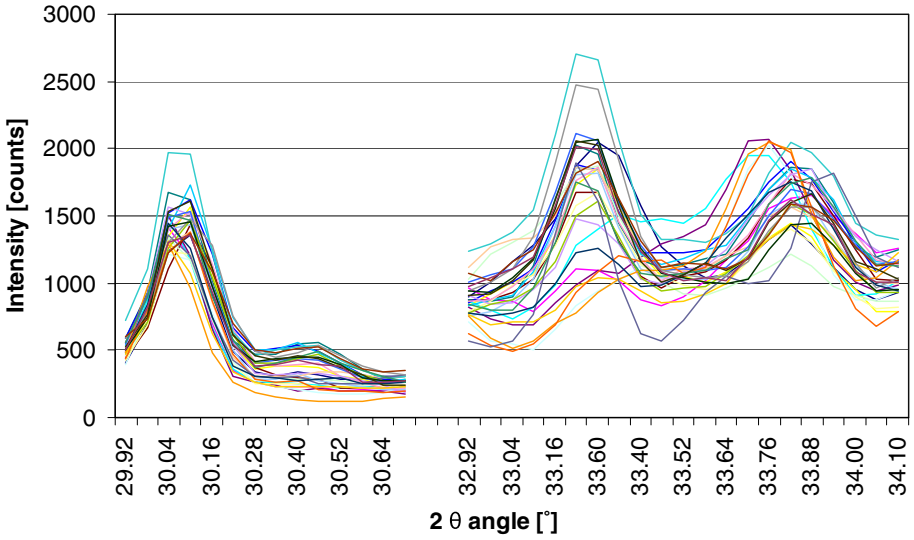

Fig. 5. The mineralogy of clinker described by XRD-profiles in the 2θ – ranges 29.88–30.70° and 32.90–34.10° of every fifth observation of totally 146 observations.

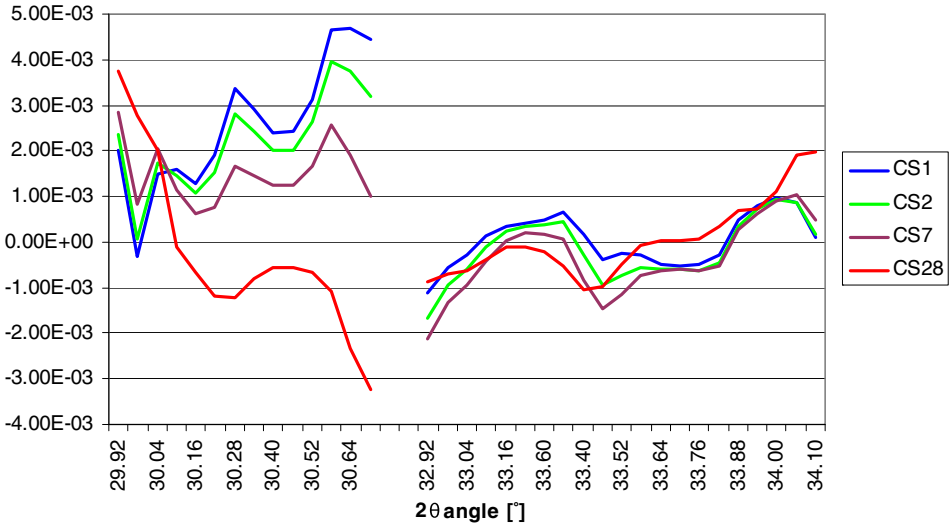

Fig. 6. The regression coefficients for prediction of compressive strength [MPa] at 1, 2, 7 and 28 d from the mineralogy of clinker described by XRD-profiles in the 2θ – ranges 29.88–30.70° and 32.90–34.10°.

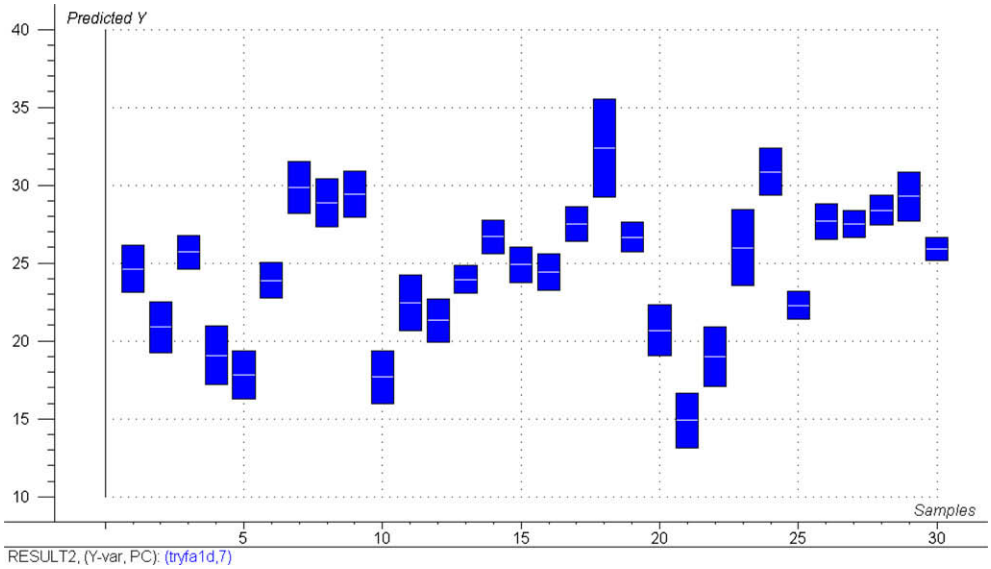

Fig. 7. Potential compressive strength [MPa] of clinker at one day predicted from the XRD-profiles in Fig 4. The confidence intervals of each y_j shown in figure is $\hat{y}_i \pm s(\hat{y}_i)$.

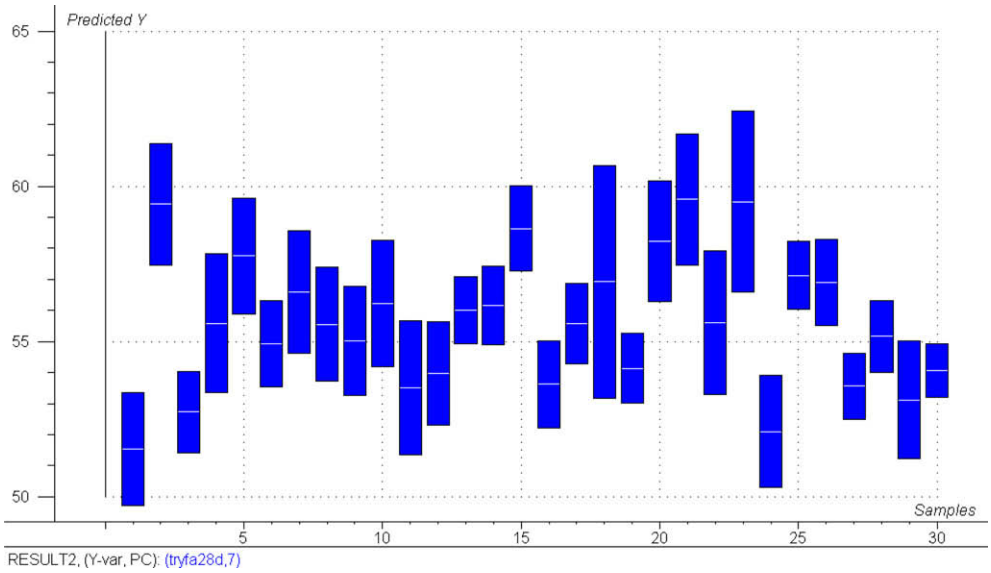

Fig. 8. Potential compressive strength [MPa] of clinker at 28 d predicted from the XRD-profiles in Fig 4. The confidence intervals of each y_j shown in figure is $\hat{y}_i \pm s(\hat{y}_i)$.

28 d, hence the variation in the two strengths predicted from the mineralogy can be said to be significant.

4.2. Examination of the influence of the mineralogy on the potential compressive strength of clinker

Including spectral variables directly in the PLS with no prior quantitative interpretation of the spectra, makes it necessary to base the sensitivity analysis on the variation of latent variables or PLS-components. The varying degree of symmetry in the shapes of the XRD-peaks and the continuity of the XRD-profile should be taken into consideration in the simulation of the variation of the *x*-variables. The fact that the mineralogy of the clinker part in the cement samples can be classified into three or four main groups, constrains the free variation of each clinker mineral. The mineralogy of about 30 out of 146 observations differed from the mineralogy of the main groups. To find the latent structure of the variables $\mathbf{x}_{\text{mineralogy}}$, a new model $y = \hat{y} = \mathbf{b}^T(\mathbf{x}_{\text{mineralogy}} \quad \mathbf{x}_{\text{suppl var}}) + b_0$ was evaluated by PLS2. $\hat{y}$ represent the predicted potential compressive strengths at 1, 2, 7 and 28 d. Some of the predicted potential compressive strengths at 1 and 28 d are presented in Figs. 7 and 8, respectively. $\mathbf{x}_{\text{mineralogy}}$ represents the XRD intensities in the 2θ – ranges 29.88–30.70° and 32.90–34.10° and $\mathbf{x}_{\text{suppl var}}$ contains the supplementary variables, the amounts of Na_2O and K_2O and the ratio Al_2O_3/Fe_2O_3. Fig. 9 shows explained variances in compressive strength at the different ages versus the number of PLS-components included in PLS2. By including predicted values of *y*, the explained variance in compressive strength at all ages was, as expected, close to 100%, in this case by including 5 PLS-components.

The simulation of the variation of the latent variables were carried out by minimizing and maximizing the potential strength at the various ages for an optimum combination of the latent variables, and in other cases the combination of the latent variables were fixed in advance. Out of the four *y*-variables included in the optimisations, one *y*-variable was selected for minimizing and

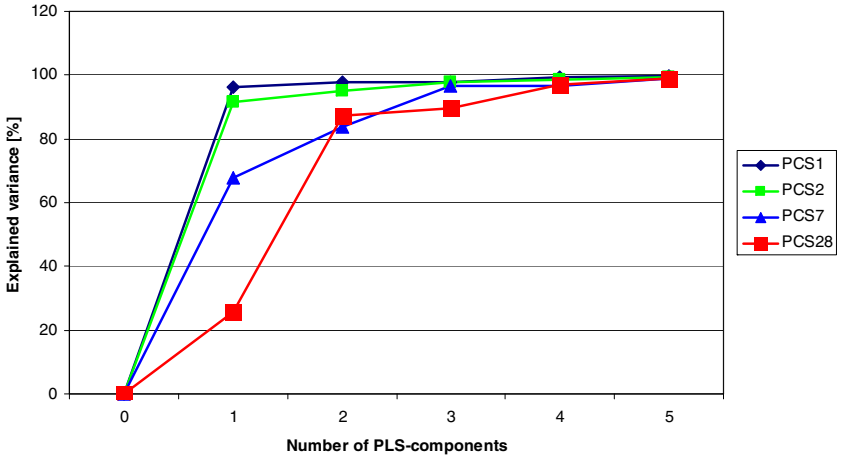

Fig. 9. Explained variances in potential compressive strength of clinker at 1, 2, 7 and 28 d from PLS2 on $\mathbf{X}_{\text{mineralogy}}$ and the supplementary variables the amounts of Na_2O, K_2O and the ratio Al_2O_3/Fe_2O_3 versus the number of PLS-components included in PLS2.

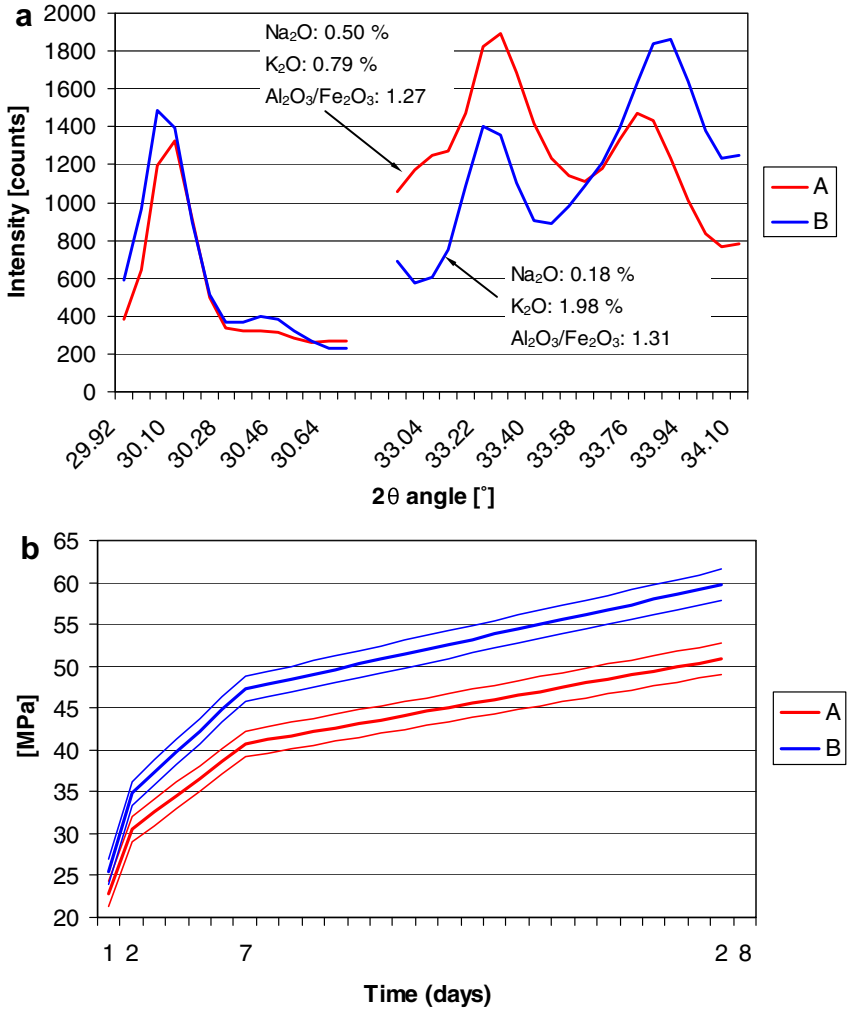

Fig. 10. Minimizing and maximizing potential compressive strength of clinker at 28 d (PCS28). (a) Optimisation of mineralogy of clinker described by the XRD-profiles in the 2θ – ranges 29.88–30.70° and 32.90–34.10° with respect to achieving min (A) and max PCS28 (B). $(n_1, n_2, n_3, n_4, n_5) = (0.001, 0.710, 0.152, 0.098, 0.004)$. (b) PCS at 1, 2, 7 and 28 d predicted from the XRD-profiles in (a). The confidence intervals of $\hat{\mathbf{y}}_i$ is $\hat{\mathbf{y}}_i \pm 1s(\hat{\mathbf{y}}_i)$.

maximizing. The other *y*-variables were predicted from the values of the *x*-variables calculated from the actual combinations of the latent variables.

Studying the explained variance in each of the four *y*-variables versus the number of latent variables included in Fig. 8, most of the explained variance in the potential compressive strengths at 1, 2

and 7 d appear to be explained by three latent variables. Explaining the potential compressive strength at 28 d, the fourth latent variable should be taken into consideration. To be sure that the absolute optimum was obtained, all five latent variables were included in the minimizing and maximizing the strength up to 28 d.

Figs. 10–13a and Fig. 13b show four cases of minimizing and maximizing potential compressive strength of clinker up to 28 d. Limits of variation of the intensities and supplementary variables, x_j, unless constrained by the latent variables, were $\bar{x}_j \pm 1.5\, s(x_j)$. The optimal combination of latent variables $(n_1, n_2, n_3, n_4, n_5)$ is given in each case of optimisation in the respective figures. As a basis for discussing the influence of the mineralogy on the potential compressive strength of clinker in the four cases of optimisation, reflections of the actual minerals in the two selected diffraction angle ranges are presented in Tables 2 and 3.

Maximizing and minimizing the potential compressive strength of clinker at 28 d (Fig. 10b) by varying the mineralogy as shown in Fig. 10a give the least change in the strength at one day. The change in strength will increase gradually up to 28 d. The change in the strength at 28 d is explained to a large extent by the shift in the C_3S-peak from 30.10° to 30.26°, indicating an increase in the amount of polymorph M_3 and a decrease in the polymorph of M_1 of C_3S [6]. M_3 has a higher birefringence than M_1 and by increasing M_3 the birefringence of alite will increase. Ono [8] has predicted the 28 d strength to increase with increasing birefringence. According to Knöfel [3] the 28 d strength increases with increasing amount of C_3S and C_3A. In accordance with [1], a decrease in the amount of C_3A ($2\theta = 33.30°$) and an increase in the amount of C_4AF contribute to an increase in the strength at 28 d. A change in the structure of the C_4AF indicated by a shift in the peak of the mineral from 33.82° to 33.94° will give an increase in the compressive strength at all the actual ages, but the highest increase in the strength occurs at 28 d. A classical example of the change in the structure of C_4AF is the one due to the change in the A/F ratio which can vary over a wide range due to a solid solution of A and F with composition C_2F as an end-point. In Fig. 10a and b, the A/F ratio is nearly constant while Na_2O decreases and K_2O increases when C_3A is decreasing. What impact do K_2O or Na_2O have on the structure of C_4AF? An increase in the amount of K_2O with a simultaneous decrease in Na_2O gives almost no change in the amount of aphthitalite, $K_3Na(SO_4)_2$ ($2\theta = 30.38°$). According to Taylor [24], a decrease in the amount of sodium could change the structure of C_3A from orthorhombic to cubic, giving a shift in the C_3A peak ($2\theta = 33.30°$) to the right. In the case depicted in Fig. 10a and b, the C_3A peak shifts slightly to the left and broadens a little when increasing Na_2O from 0.18% to 0.50%. According to

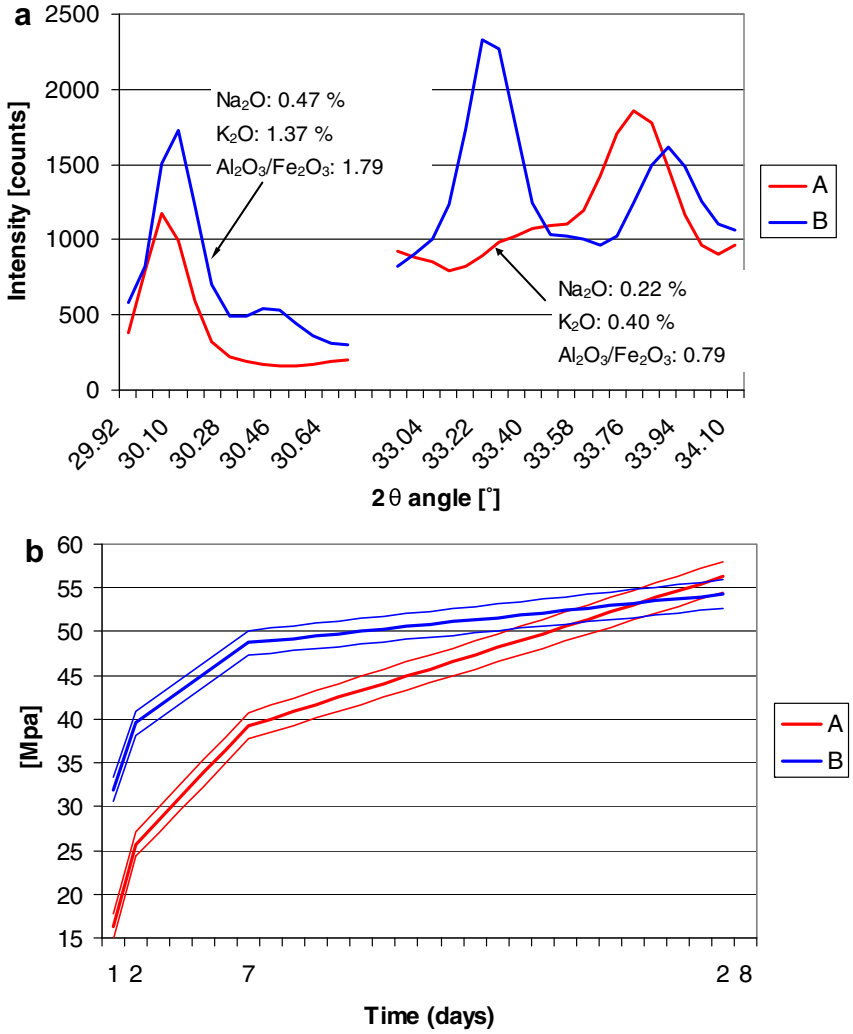

Fig. 11. Minimizing and maximizing potential compressive strength of clinker at 1 d (PCS1). (a) Optimisation of mineralogy of clinker described by the XRD-profiles in the 2θ – ranges 29.88–30.70° and 32.90–34.10° with respect to achieving min (A) and max PCS1 (B). $(n_1, n_2, n_3, n_4, n_5) = (0.717, 0.054, 0.090, 0, 0.138)$. (b) PCS at 1, 2, 7 and 28 d predicted from the XRD-profiles in (a). The confidence intervals of $\hat{\mathbf{y}}_i$ is $\hat{\mathbf{y}}_i \pm 1s(\hat{\mathbf{y}}_i)$.

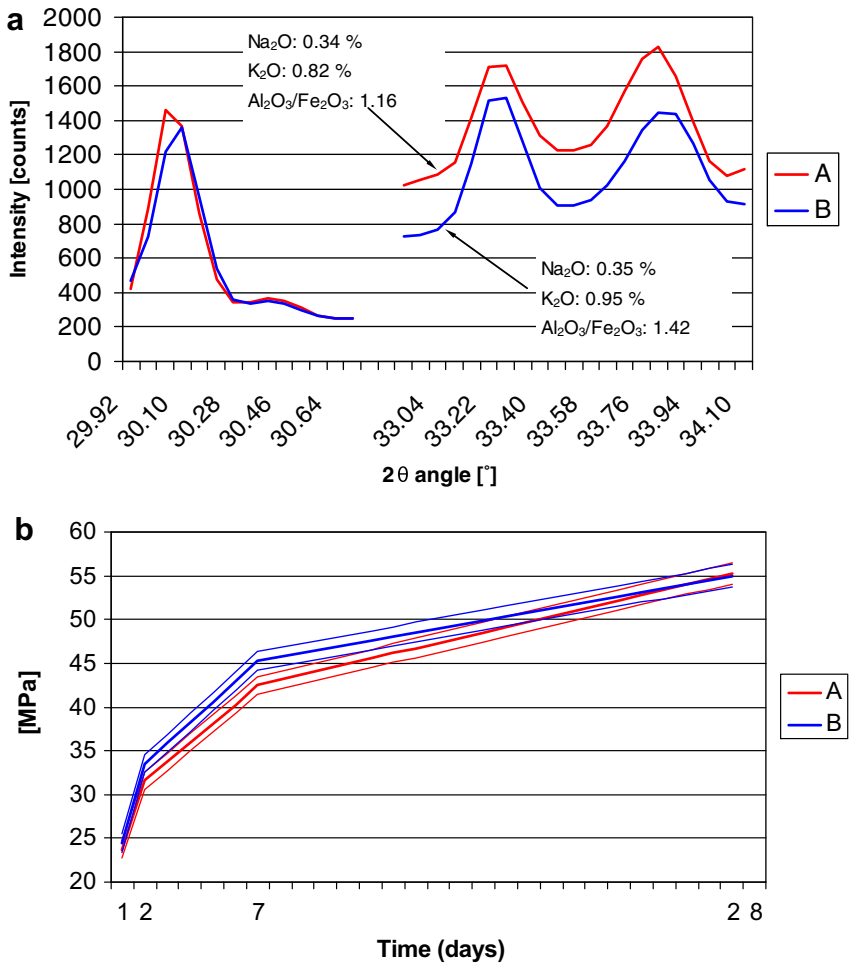

Fig. 12. Minimizing and maximizing potential compressive strength of clinker at 7 d (PCS7). (a) Optimisation of mineralogy of clinker described by the XRD-profiles in the 2θ – ranges 29.88–30.70° and 32.90–34.10° with respect to achieving min (A) and max PCS7 (B). $(n_1, n_2, n_3, n_4, n_5) = (0, 0, 1, 0, 0)$. (b) PCS at 1, 2, 7 and 28 d predicted from the XRD-profiles in (a). The confidence intervals of $\hat{\mathbf{y}}_i$ is $\hat{\mathbf{y}}_i \pm 1s(\hat{\mathbf{y}}_i)$.

Odler and Wonnemann [6] the development of strength is not altered significantly due alkali oxides being incorporated into the crystalline lattice of clinker minerals.

Maximizing and minimizing potential compressive strength of clinker at 1 d (Fig. 11a) by varying the mineralogy as shown in Fig. 11b, give the highest change in the strength at 1 d and no change in the strength at 28 d. Comparing the change in the microstructure described by XRD-profiles with the regression coefficients, $\mathbf{b}_w$, in [1] shows that the increase in compressive strength at one day can be explained by:

- An increase in the amount of and also the shift in the structure of C_3S.
- An increase in the amount of aphthitalite.
- An increase in the amount of C_3A.
- A change in the structure of C_4AF indicated by a shift in the peak to the left.

Lawrence [4] has predicted the strength at 1 d to increase with increasing C_3S but decrease with increasing C_3A. The increase in strength at 1 d with increasing amount of aphtitalite predicted in this work contradicts what is observed by Odler and Wonnemann [7]; a decrease in strength with increases in the amounts of Na_2SO_4 and K_2SO_4 in cement. The change in the mineralogy described by the XRD-profile in the 2θ – ranges 32.90–34.10° is to a large extent identical to the difference in the mineralogy between standard Portland cement and low alkali, sulphate resistant cement [2]. The change in the structure of C_4AF by increasing A/F ratio is evident.

In the case of the optimisation presented in Fig. 12a and b) the combination of latent variables was fixed in advance to $(n_1, n_2, n_3, n_4, n_5) = (0, 0, 1, 0, 0)$. An interesting result is the variation in the potential compressive strength of clinker at 2 and 7 d while no significant change in the potential compressive strengths was found at 1 and 28 d. The change in strength at 2 and 7 d can only be explained by a change in the structure of C_3S and a decrease of C_3A and C_4AF. Aldridge [5] has predicted the strength at 7 d to increase with increases in both C_3S and C_3A. The influence of C_3A on the strength at 7 d is higher than influences on strengths at earlier ages.

In the last case of optimisation (Fig. 13a and b), the amount of Na_2O was kept constant. The optimisation from state A to B gave significant increase in compressive strength at all the ages, but highest increase in the strength at 2 and 7 d. The change in the strength can best be explained by changes in the amount of C_3S, aphthitalite and C_3A. Optimisation by keeping the amount of K_2O and A/F ratio constant gave no change in the mineralogy and consequently no change in the compressive strength at any of the ages.

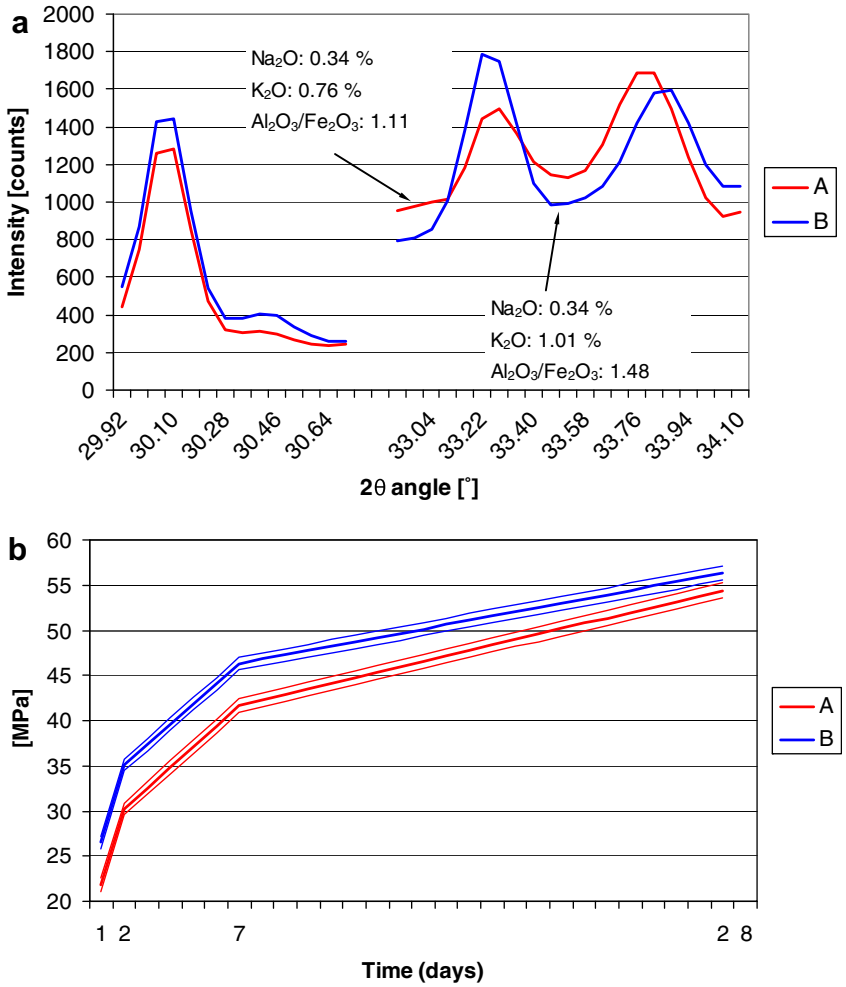

Fig. 13. Minimizing and maximizing potential compressive strength of clinker at 28 d (PCS28), keeping the amount of Na_2O constant. (a) Optimisation of mineralogy of clinker described by the XRD-profiles in the 2θ – ranges 29.88–30.70° and 32.90–34.10° with respect to achieving min (A) and max PCS7 (B). Na_2O was kept constant and equal to 0.34%. $(n_1, n_2, n_3, n_4, n_5) = (0.309, 0.255, 0.167, 0.134, 0.134)$. (b) PCS at 1, 2, 7 and 28 d predicted from the XRD-profiles in (a). The confidence intervals of $\hat{\mathbf{y}}_i$ is $\hat{\mathbf{y}}_i \pm 1s(\hat{\mathbf{y}}_i)$.

Table 2
Major phases within the XRD range $2\theta = 29.88–30.70°$.

Phase	2θ (°)	d (nm)	Indices ⟨hkl⟩	Intensity (rel)
Alite (M_3)	30.04	0.2975	⟨804⟩	10
	30.09	0.2970	⟨620⟩	20
Aphthitalite	30.38	0.2940	⟨102⟩	75

Table 3
Major phases within the range $2\theta = 32.90–34.10°$.

Phase	2θ (°)	d (nm)	Indices ⟨hkl⟩	Intensity (rel)
Belite, β-C_2S	32.98	0.2716	⟨121⟩	38
α′- C_2S	33.65	0.2663	⟨260⟩	100
Cubic C_3A	33.26	0.2694	⟨044⟩	100
Orthorhombic C_3A	33.27	0.2693	⟨224⟩	100
	33.04	0.2711	⟨040⟩	25
	32.93	0.2720	⟨400⟩	31
$C_{12}A_7$	33.41	0.2680	⟨420⟩	100
C_4AF	33.84	0.2649	⟨141⟩	100
	33.64	0.2664	⟨002⟩	47
Gypsum	33.35	0.2684	⟨150⟩ and ⟨220⟩	50

Applying experimental design in the build-up of the observation matrix could reveal to a greater extent the impact of the separate clinker phases on the compressive strength development.

5. Conclusions

Potential compressive strength of clinker can be predicted from the mineralogy of clinker on the basis of a statistical model for prediction of compressive strength up to 28 d from the microstructure of cement.

It has been shown that prediction of potential compressive strength of clinker up to 28 d from the observed variation in the mineralogy gave significant variation of the strength at both 1 and 28 d.

Sensitivity analysis based on simulation, optimisation and prediction made it possible to study the influence of the mineralogy on the strength in more detail.

In minimizing and maximizing the potential compressive strength at one day, the variables describing the amounts of C_3S and aphthitalite were found to be the most influential.

Change in the structure of C_3S indicated by a shift in its XRD-peak in the selected 2θ – ranges influenced the potential compressive strength at 28 d significantly.

References

[1] Svinning K, Høskuldsson A, Justnes H. Prediction of compressive strength up to 28 d from microstructure of Portland cement. Cem. Concr Compos 2008;30:138–51.
[2] Svinning K, Justnes H, Viggh E, Bremseth SK, Johansson S-E. Examination of clinkers from four Scandinavian plants with respect to microstructure and cement properties. In: Proceedings of the 22nd international conference on cement microscopy, Montreal; 2000. p. 137–53.
[3] Knöfel D. Interrelation between proportion of clinker phases and compressive strength of Portland cements. In: Proceedings of the 11th international conference on cement microscopy, New Orleans; 1989. p. 246–62.
[4] Lawrence CD. A study of the microstructure of hardened cement paste by nitrogen and butane sorbtion, PhD thesis, Brunel University; 1981.
[5] Aldridge LP. Estimating strength from cement composition. In: Proceedings of the 7th international congress on the chemistry of cement, Paris; 1980 (Communication: vol. III, VI-83-6).
[6] Odler I, Wonnemann R. Effects of alkalis on Portland cement hydration I. Alkali oxides incorporated into the crystalline lattice of clinker minerals. Cem Concr Res 1983;13:477–82.
[7] Odler I, Wonnemann R. Effects of alkalis on Portland cement hydration. II. Alkalis present in forms of sulfates. Cem Concr Res 1983;13:771–7.
[8] Ono Y. 1995, Presented in Campbell DH, microscopical examination and interpretation of Portland cement and clinker. 2nd ed. Skokie: Portland Cement Association; 1999.
[9] Ono Y. Lattice Constants of alite in plant clinker. In: Review of the 38th general meeting, technical session. Tokyo: The Cement Association of Japan; 1984. p. 28–31.
[10] Dunstetter F, de Noirfontaine M-N, Courtial M. Polymorphism of tricalcium silicate, the major compound of Portland cement clinker, 1. Structural data: review and unified analysis. Cem Concr Res 2006;36:39–53.
[11] Maki I, Chromy S. Characterization of the alite phase in Portland cement clinker by microscopy. Il Cemento 1978;3:301–8.
[12] Maki I, Kato K. Phase identification of alit in Portland cement clinker. Cem Concr Res 1982;12:93–100.
[13] Svinning K, Høskuldsson A. Prediction of potential compressive strength of Portland clinker from production condition cement kiln. J ASTM Int., submitted for publication.
[14] Akkurt S, Tayfur G, Sever C. Fuzzy logic model for the prediction of cement compressive strength. Cem Concr Res 2004;34:1429–33.
[15] Tsivillis S, Parissakis G. A mathematical model for prediction of cement strength. Cem Concr Res 1988;28:9–14.
[16] Akkurt S, Ozdemir S, Tayfur G, Akyol B. The use of GA-ANN in the modelling of compressive strength of cement mortar. Cem Concr Res 2003;33:973–80.
[17] Baykasoglu A, Türkay D, Serkan T. Prediction of cement strength using soft computing techniques. Cem Concr Res 2004;34:2083–90.
[18] Svinning K, Bremseth SK, Justnes H. X-ray diffraction studies on variations in microstructure of Portland clinker correlated with variations in production conditions in the kiln. World Cem 1996:80–6.
[19] Svinning K, Bremseth SK. The influence of microstructure of clinker and cement on setting time and strength development until 28 d. In: Proceedings of 18th international conference on cement microscopy, Houston; 1996. p. 514–13.
[20] Svinning K, Justnes H. Application of partial least square regression analysis in examination of correlations between production conditions, microstructure of clinker and cement and cement properties. In: Proceedings of the 10th international congress on the chemistry of cement, Gothenburg; 1997, li038. p. 8.
[21] Svinning K. Design and manufacture of Portland cement – application of sensitivity analysis in exploration and optimization. Part I: Exploration. J Chemometr Intell Lab Sys 2006;84:177–87.
[22] Svinning K, Høskuldsson A. Design and manufacture of Portland cement – application of sensitivity analysis in exploration and optimization. Part II: Optimization. J Chemometr Intell Lab Sys 2006;84:188–94.
[23] Martens H, Næs T. Multivariate calibration. 2nd ed. Chichester: Wiley; 1989.
[24] Taylor HFW. Cement chemistry. 1st ed. London: Academic Press; 1990. p. 24.